Asian Journal of Physics Vol. 20, No. 4 (2011) 403-423

Density functional theory computations on vibrational spectra: Scaling procedures to improve the results

M Alcolea Palafox[a], V K Rastogi[b] and Kaushal Rani[c]
[a]*Departamento de Química-Física I. Facultad de Ciencias Químicas Universidad Complutense, Madrid- 28040-ES. SPAIN*
[b]*Department of Physics, CCS University Campus, Meerut-250004, India.*
[c]*Indian Spectroscopy Society, K C 68/1 Old Kavi Nagar, Ghaziabad-201 002, India*

The basic Density Functional Theory (DFT) was described, and the most common density functionals were listed. The performance of ab initio and DFT methods in calculating the geometric parameters and vibrational frequencies was analyzed. The accuracy of the results in the isolated state, as well as in the solid state was shown in the IR and Raman spectra. To correct the calculated frequencies, several scaling procedures were described in detail. A comprehensive compendium of the mainly scale factors available to date for a good accurate prediction of the frequencies was also shown. Examples of each case were presented, with special attention to the benzene and uracil molecules and to some of their derivatives.

1. Introduction

Density functional theory (DFT) has become very popular in recent years. This is justified based on the pragmatic observation that it is less computationally intensive than other methods with similar accuracy, or even better in some cases, such as the theoretical prediction of vibrational spectra. The most accurate of the quantum chemical methods are still too expensive and cumbersome to apply as routine research. For this reason, we show in the present paper an overview of the description and advantages in the use of DFT methods in vibrational spectroscopy.

The last decade has been highly productive in the interpretation of vibrational experimental spectra by means of quantum chemical methods, in especial by DFT methods. The theoretical prediction of vibrational spectra has been of practical importance for the identification of known and unknown compounds, and has become an important part of spectrochemical and quantum chemical investigations. The reliable prediction of the vibrational spectra, particularly in synthetic and natural product chemistry, can be used to calculate the expected spectra of proposed structures, confirming the identity of a product or of a completely new molecule.

DFT methods can also be used to help in the assignment of the bands of the spectra. Until recently, chemical spectroscopists have attempted to interpret the vibrational spectra of more complex molecules by a transposition of the results of normal coordinate analysis of simpler molecules, often aided by qualitative comparisons of the spectra of isotopically substituted species, and the polarizations of the Raman bands. Thus, it has become an accepted practice to include tables of these "vibrational assignments" in publications on the infrared and Raman spectra of larger molecules. However, to make such "assignments" for all the bands in the spectra is risky, owing to the fact that while some of the assignments may be credible, other can be highly speculative. Further, the modes assigned to these vibrations are often grossly oversimplified in an attempt to describe them as group wavenumbers in localized bond systems. The use of adequate DFT quantum-chemical methods and scaling procedures, remarkably reduce the risk in the assignment and can accurately determine the contribution of the different modes in an observed band. Now this procedure appears to be used extensively in the journals of vibrational spectroscopy.

Corresponding author :
e-mail: alcolea @quim.ucm.es-(Prof M A Palafox);*v_krastogi@rediffmail.com* (Prof V K Rastogi)

The computation of the vibrational spectrum of a polyatomic molecule of even modest size is lengthy. In spite of the tremendous advances made both in theoretical methods, in special with DFT methods and computer hardware. One may be forced to work at a low level, and consequently, one must expect a large overestimation of the calculated vibrational wavenumbers. This overestimation (which may be due to many different factors that are usually not even considered in the theory, such as anharmonicity, errors in the computed geometry, Fermi resonance, solvent effects, etc) can be remarkably reduced with the use of transferable empirical parameters for the force fields, or for the calculated wavenumbers. The scale factor is therefore designed to correct the calculated harmonic wavenumbers to be compared with the anharmonic wavenumbers found by the experiment. The scale factor is a consequence of the deficiency of the theoretical approach and potentially allows vibrational wavenumbers (and thermochemical information) of useful accuracy to be obtained from procedures of modest computational cost only. Widespread application to molecules of moderate size is then possible.

One of the goals of the present work was try to resume the different procedures used for scaling and the accuracy reached with them. As examples, we show the results with several benzene and uracil derivatives.

2. Basic DFT theory

The premise behind DFT is that the energy of a molecule can be determined from the electron density instead of a wave function. This theory originated with a theorem by Hoenburg and Kohn that stated this was possible. A practical application of this theory was developed by Kohn and Sham who formulated a method similar in structure to the Hartree-Fock method[1-4].

In this formulation, the electron density is expressed as a linear combination of basis functions similar in mathematical form to HF orbitals. A determinant is then formed from these functions, called Kohn-Sham orbitals. It is the electron density from this determinant of orbitals that is used to compute the energy. This procedure is necessary because Fermion systems can only have electron densities that arise from an antisymmetric wave function. There has been some debate over the interpretation of Kohn-Sham orbitals. It is certain that they are not mathematical equivalent to either HF orbitals or natural orbitals from correlated calculations. However, Kohn-Sham orbitals do describe the behavior of electron in a molecule, just as the other orbitals mentioned do. DFT orbitals eigenvalues do not match the energies obtained from photoelectron spectroscopy experiments as well as HF orbitals energies do. The questions still being debated are how to assign similarities and how to physically interpret the differences.

In DFT the exact exchange (HF) for a single determinant is replaced by a more general expression, the exchange-correlation functional, which can include terms accounting for both exchange energy and the electron correlation, which is omitted from Hartree-Fock theory. The energy has the form:

$$E_{ks} = V + \langle hP \rangle + \tfrac{1}{2} \langle PJ(P) \rangle + E_x[P] + E_c[P]$$

where the terms have the following meanings:

V is the nuclear repulsion energy, P is the density matrix, $\langle hP \rangle$ is the one-electron (kinetic plus potential) energy, $\tfrac{1}{2} \langle PJ(P) \rangle$ is the classical coulomb repulsion of the electrons, $E_x[P]$ is the exchange functional, and $E_c[P]$ is the correlation functional.

A density functional is then used to obtain the energy from the electron density[1]. A functional is a function of a function, in this case, the electron density. The exact density functional is not known. Therefore, there is a whole list of different functionals that may have advantages or disadvantages. Some of these functionals were developed from fundamental quantum mechanics and some were developed by

parameterizing functions to best reproduce experimental results. Thus, there are in essence ab initio and semiempirical versions of DFT. Thus, DFT tends to be classified either as an ab initio method or in a class by itself.

The advantage of using electron density is that the integrals for Coulomb repulsion need be done only over the electron density, which is a three-dimensional function, thus scaling as N^3. Furthermore, at least some electron correlation can be included in the calculation. This results in faster calculations than HF calculations (which scale as N^4) and computations that are a bit more accurate as well. The better DFT functionals give results with accuracy similar to that of an MP2 calculation.

Density functionals can be broken down into several classes. The simplest is called the Xα method. This type of calculation includes electron exchange but not correlation. It was introduced by J.C. Slater, who in attempting to make an approximation to Hartree-Fock unwittingly discovered the simplest form of DFT. The Xα method is similar in accuracy to HF and sometimes better.

The simplest approximation to the complete problem is one based only on the electron density, called a local density approximation (LDA). For high-spin systems, this is called the local spin density approximation (LSDA). LDA calculations have been widely used for band structure calculations. Their performance is less impressive for molecular calculations, where both qualitative and quantitative errors are encountered. For example, bonds tend to be too short and too strong. LDA, LSDA, and VWN (the Vosko, Wilks, and Nusair functional) have become synonymous in the literature.

A more complex set of functionals utilizes the electron density and its gradient. These are called gradient-corrected methods. There are also hybrid methods that combine functionals from other methods with pieces of a Hartree-Fock calculation, usually the exchange integrals.

In general, gradient-corrected or hybrid calculations give the most accurate results. However, there are a few cases where Xα and LDA do quite well. LDA is known to give less accurate geometries and predicts binding energies significantly too large. The current generation of hybrid functionals is a bit more accurate than the gradient-corrected techniques. Some of the more widely used functionals are listed in Table 1.

Table 1. The most common Density functionals used today.

Acronyms	Name	Type
Xα	X-alpha	Exchange only
HFS	Hartree-Fock Slater	HF with LDA exchange
VWN	Vosko, Wilks, and Nusair	LDA
BLYP	Becke correlational functional with Lee, Yang, Parr exchange Becke 3 term with Lee, Yang, Parr exchange	Gradient-corrected
B3LYP	Perdue and Wang 1991	Hybrid
PW91	Gill 1996	Gradient-corrected
G96	Perdew 1986	Exchange
P86	Becke 1996	Gradient-corrected
B96	Becke exchange, Perdew correlation	Gradient-corrected
B3P86	Becke exchange, Perdew and Wang correlation	Hybrid
B3PW91		Hybrid

DFT is generally faster than Hartree-Fock for systems with more than 10-15 non-hydrogen atoms[1], depending on the numeric integral accuracy and basis set. DFT calculations must use a basis set. Most

DFT calculations today are being done with HF-optimized GTO basis sets. The accuracy of results tends to degrade significantly with the use of very small basis sets. For accuracy considerations, the smallest basis set used is generally 6-31G* or the equivalent. Interestingly, there is only a small increase in accuracy obtained by using very large basis sets. This is probably due to the fact that the density functional is limiting accuracy more than the basis set limitations.

The accuracy of results from DFT calculations can be poor to fairly good, depending on the choice of basis set and density functional[1]. The choice of density functional is made more difficult because creating new functionals is still an active area of research. In DFT methods, the most prominent are B-LYP and B3-LYP. B-LYP uses a combination of the Becke exchange functional[5] (B) coupled with the correlational functional of Lee, Yang and Parr[6] (LYP), while the hybrid B3-LYP procedure uses Becke's three-parameter exchange functional[7] (B3), in combination with the LYP correlation functional. The B and B3 exchange functional can be used with other correlation functionals[8,9] such as P86 and PW91 to compute vibrational frequencies, although they have received less attention in the recent literature. The B3LYP hybrid functional (also called Becke3LYP) was the most widely used for molecular calculations by a fairly large margin. This is due to the accuracy of the B3LYP results obtained for a large range of compounds, particularly organic molecules.

Due to the newness of DFT, its performance is not completely known and continues to change with the development of new functionals. At the present time, DFT results have been very good for organic molecules, particularly those with closed shells. Results have not been so encouraging for heavy elements, highly charged systems, or systems known to be very sensitive to electron correlation. Also, the functionals listed in Table 1 do not perform well for problems dominated by dispersion forces. Unfortunately, there is no systematic way to improve DFT calculations, thus making them unusable for very-high-accuracy work.

3. Basis Set

A basis set is a set of functions used to describe the shape of the orbitals in an atom. Molecular orbitals and entire wave functions are created by taking linear combinations of basis functions and angular functions. Most semiempirical methods use a predefined basis set. When ab initio or DFT calculations are done, a basis set must be specified. Although it is possible to create a basis set from scratch, most calculations are done using existing basis sets. The type of calculation performed and basis set chosen are the two biggest factors in determining the accuracy of results[1].

There are several types of basis functions. Over the past several decades, most basis sets have been optimized to describe individual atoms at the HF level of theory. There have been a few basis sets optimized for use with DFT calculations, but these give little if any increase in efficiency over using HF optimized basis set. In general, DFT calculations do well with moderate-size HF basis sets and show a significant decrease in accuracy when a minimal basis set is used. Also, DFT calculations show only a slight improvement in results when large basis sets are used. This seems to be due to the approximate nature of the DFT limiting accuracy more than the lack of a complete basis set[1].

Several basis schemes are used for very high accuracy calculations. The highest accuracy HF calculations use numerical basis sets, usually a cubic spline method. For high accuracy correlated calculations with an optimal amount of computing effort, correlation-consistent basis sets have mostly replaced Atomic Natural Orbital (ANO) basis sets. Complete basis set, or CBS, calculations go a step beyond this in estimating the infinite basis set limit.

Below is a listing of some of the commonly used basis sets:

- *STO-nG* (n = 2-6) n primitives per shell per occupied angular momentum (*s*,*p*,*d*). It is the most widely used minimal basis set.

- *6-31G* Pople sets, particularly 6-31G and 6-311G. They are the most popular for quantitative results in organic molecules. Available in general for H(4*s*) through Ar (16*s*10*p*).
- *Dunning-Hay* sets. They are in general available for H(4*s*) through Ne.
- *cc-pVnZ* (n = D, T, Q, 5, 6) Correlation-consistent basis sets that always include polarization functions. They are in general available for H through Ar. The various sets describe H with from (2*s*1*p*) to (5*s*4*p*3*d*2*f*1*g*) primitives. One to four diffuse functions are denoted with the notation *aug* or *n-aug*, where *n = d, t, q*.
- *cc-pCVnZ* (n = D, T, Q, 5) Correlation-consistent basis sets designed to describe the correlation of the core electrons as well as the valence electrons. Available for H through Ne. These basis sets were created from the cc-pVnZ sets by adding from 2 to 14 additional primitives starting at the inner shells.
- *CBS-n* (n = 4, Lq, Q, APNO) For estimating the infinite basis set limit. This implies a series of calculations with different basis sets, some of which are large sets. The CBS and G2 methods are becoming popular for very-high accuracy results. Available for H through Ne.
- *DZVP, DZVP2, TZVP*. DFT-optimized functions. Available for H through Xe.
- *Hay*. The larger set is popular for transition metal calculations. Available for Sc through Cu(12*s*6*p*4*d*) and (14*s*9*p*5*d*).
- *Wachters*. Often used for transition metals. Available for K through Zn(14*s*9*p*5*d*).

There are many more basis set developed, some of them were the work of many different authors and later improved. This sometimes results in different programs using the same name for two slightly different sets. It is also possible to combine basis sets of modify them, which can result in either poor or excellent results, depending on how expertly it is done.

4. Frequency Calculation

Because of the nature of the computations involved, frequency calculations are valid only at stationary points on the potential energy surface. Thus, they must be performed on optimized structures. For this reason, it is necessary to run a geometry optimization prior to making a frequency calculation. To ensure that a real minimum is located on the potential energy surface, imaginary values should not appear among the calculated harmonic frequencies.

A frequency job must use the same theoretical model and basis set as employed in the optimized geometry. Frequencies computed with different basis sets or procedures have no validity. A frequency job begins by computing the energy of the input structure. It then goes on to minimize this energy and recalculate a new geometry. The process is successively repeated until the change in the forces and in the displacements of the atoms of the molecule, is lower than a certain fixed threshold. When it is reached, the geometry corresponds to an optimum structure and then the frequencies can be computed. The frequencies, intensities, Raman depolarization ratios and scattering activities for each spectral line are therefore predicted. However, calculated values of the intensities should not be taken too literally, due to the high error in their computation, although relative values of the intensities for each frequency may be reliably compared.

In addition to the frequencies and intensities, the output of the free and commercial quantum chemical programs also displays the atomic displacements for each computed frequency. These displacements are presented as XYZ coordinates, in the standard orientation, which can be plotted to identify each vibration[10].

5. Error in the geometric parameters

Previously to the frequency calculations it is necessary a full optimization of the molecule. As example, in Table 2 is shown the calculated bond lengths of benzene and aniline molecules by different ab initio and DFT methods, that can be compared to the experimental data reported by x-ray, microwave (MW) and electron diffraction (ED). This last technique gives the molecular structure in the gas phase, which are more close to our calculated values than x-ray or MW. Thus, when ED data are available, the comparison of the theoretical values should be carried out with this technique. Can be seen the close value of the DFT results to the experimental ones, especially by B3LYP. The accuracy is almost similar to that by MP2.

Table 2. Optimum bond lengths in A for the benzene and aniline molecules

	benzene		aniline							
Methods	C-C	C-H	C1-C2 (C1-C6)	C2-C3 (C5-C6)	C3-C4 (C4-C5)	C1-N	C2-H (C6-H)	C3-H (C5-H)	C4-H	N-H
SCF and Post-SCF methods										
HF/6-31G[a]	1.3862	1.0756	1.395	1.389	1.389	1.401	1.072	1.072	1.070	0.997
HF/6-31G*	1.3859	1.0760	1.393	1.383	1.386	1.397	1.077	1.076	1.075	0.997
HF/6-31G**	1.3883	1.0758	1.3928	1.3831	1.3853	1.3947	1.0768	1.0763	1.0750	0.9956
HF/6-31++G**			1.3939	1.3852	1.3873	1.3953	1.0767	1.0761	1.0748	0.9959
MP2/6-31G*	1.3963	1.0827	1.4023	1.3942	1.3963	1.4067	1.0889	1.0877	1.0866	1.0151
MP2/6-31G**	1.3979	1.0832	1.4019	1.3937	1.3958	1.4056	1.0842	1.0829	1.0819	1.0103
MP2/6-31G(2d,p)			1.4021	1.3953	1.3972	1.4081	1.0847	1.0834	1.0823	1.0108
MP2/6-311G(2d,p)			1.4003	1.3928	1.3948	1.4057	1.0870	1.0855	1.0845	1.0125
Density functional methods										
BP86/6-31G**	1.4044	1.0952	1.4145	1.4004	1.4045	1.4021	1.0965	1.0954	1.0940	1.0194
BP86/6-311G(2d,p)	1.3992	1.0929	1.4091	1.3954	1.3994	1.4028	1.0944	1.0931	1.0917	1.0190
BLYP/6-31G**	1.4065	1.0934	1.4163	1.4026	1.4065	1.4091	1.0945	1.0936	1.0923	1.0197
B3P86/6-31G*	1.3932	1.0867	1.4021	1.3897	1.3931	1.3925	1.0879	1.0869	1.0856	1.0111
B3P86/6-31G**	1.3929	1.0860	1.4022	1.3893	1.3929	1.3902	1.0872	1.0863	1.0849	1.0092
B3LYP/6-31G*	1.3964	1.0866	1.4052	1.3931	1.3965	1.4004	1.0881	1.0872	1.0860	1.0129
B3LYP/6-31G**	1.3963	1.0863	1.4054	1.3928	1.3962	1.3981	1.0875	1.0866	1.0853	1.0866
B3LYP/6-311G(2d,p)	1.3911	1.0838	1.4000	1.3877	1.3911	1.3988	1.0851	1.0841	1.0827	1.0102
B3LYP/6-311+G(2d,p)	1.3914	1.0836	1.3996	1.3887	1.3918	1.3997	1.0850	1.0840	1.0827	1.0098
B3LYP/6-311++G(2df,2p)			1.3994	1.3878	1.3912	1.3951	1.0832	1.0821	1.0808	1.0067
B3LYP/6-311++G(3df,pd)			1.3990	1.3875	1.3907	1.3954	1.0841	1.0831	1.0818	1.0089
B3PW91/6-31G**	1.3945	1.0868	1.4038	1.3908	1.3943	1.3920	1.0878	1.0869	1.0856	1.0094
Experimental										
x-ray[b]	1.3920[e]	1.0862[e]	1.404 (6)	1.380 (7)	1.386 (7)	1.398 (6)	1.03 (3)	0.95 (4)	1.05 (5)	1.07 (5)
MW[c]			1.397 (3)	1.394 (4)	1.396 (2)	1.402 (2)	1.082 (4)	1.083 (2)	1.080 (2)	1.001 (10)
ED[d]			1.403 (3)	1.3933(1)	1.3955(1)	1.4057(1)	1.099 (3)	1.099 (3)	1.099 (3)	1.021 (1)

[a]From ref. 12. [b]From ref. 13 [c]From ref. 14. [d]From ref. 15 [e]r_m value, refs. [16].

Table 3 shows the calculated bond angles and torsional angles in the aniline molecule by different ab initio and DFT methods. Also can be seen the low errors obtained using DFT methods.

Table 3. Calculated and experimental bond angles and torsional angles, in degrees, in aniline molecule

Methods	C1 C2 C3 (1 6 5)	C2 C3 C4 (4 5 6)	C3 C4 C5	C2 C1 C6	C2 C1 N (C6 C1 N)	C N H	H N H	α (tilt angle)	ω (inversion)	C3 C2 C1 N	C2 C1 N H
SCF and Post SCF methods											
HF/6 31G**	120.39	120.88	118.74	118.71	120.62	112.64	111.35	2.16	42.30	27.73	25.88
HF/6 31++G**	120.38	120.88	118.73	118.76	120.60	112.60	111.56	2.54	41.28	27.68	25.45
MP2/6 31G*	120.43	120.58	119.13	118.84	120.49	113.09	109.74	4.21	41.03	26.64	29.70
MP2/6 31G**	120.43	120.56	119.16	118.84	120.47	113.01	109.71	4.31	41.18	26.68	30.01
MP2/6 31G(2d,p)	120.56	120.50	119.17	118.71	120.55	112.79	109.16	3.06	48.69	26.60	30.31
MP2/6 31G(2d,2p)	120.61	120.50	119.13	118.64	120.61	112.60	109.61	3.38	48.19	26.39	29.89
Density functional methods											
B3P86/6 31G**	120.49	120.82	118.87	118.51	120.70	112.65	111.33	2.65	42.30	26.87	26.26
B3P86/6 31G(2d,p)	120.55	120.78	118.89	118.45	120.73	112.02	110.78	2.92	41.23	26.58	27.44
B3LYP/6 31G**	120.47	120.79	118.93	118.61	120.66	112.50	111.09	2.61	42.89	26.86	26.64
B3P86/6 31G**	120.50	120.83	118.87	118.50	120.72	112.13	111.93	2.30	40.64	27.32	25.11
B3LYP/6 31G**	120.48	120.80	118.88	118.56	120.69	112.48	111.50	2.38	41.71	27.20	25.17
B3LYP/6 31G(2d,p)	120.53	120.76	118.90	118.50	120.71	112.23	110.90	2.21	43.64	26.82	27.04
B3LYP/6 31G(2d,2p)	120.48	120.75	118.91	118.63	120.65	112.97	111.48	2.51	42.12	27.10	25.78
B3LYP/6 31G(2df,2p)	120.49	120.77	118.89	118.59	120.68	112.82	112.30	2.39	38.57	27.21	24.11
B3LYP/6 31G(3df,3pd)	120.51	120.78	118.87	118.56	120.69	112.50	111.96	2.47	39.69	27.25	24.19
B3PW91/6 31G**	120.51	120.83	118.83	118.48	120.73	112.13	111.87	2.32	40.70	27.31	25.17
Experimental											
x ray[a]	119.7 (4)	122.1 (5)	117.6(5)	117.9(4)	120 (3)	119 (4)			42.3		
MW[b]	120.12(2B)	120.70(8)	118.92(8)	119.43(20)	120.28(2.0)	112.9	111.1(2.0)[c]	4.6	42.5[d]		
ED[e]	120.28(30)	120.69(4)	119.03(14)	119.01(16)	120.45(8)				[f]		

[a] From ref. 13. [b] From ref. 14. [c] From ref. 15. [d] 111.15 ± 0.03° in ref. 17. [e] From ref. 17.

6. Error in the calculated frequencies

The vibrational frequencies are usually calculated using the simple harmonic oscillator model. Therefore, they are typically larger than the fundamentals observed experimentally[9]. The possible reasons for the deficiency of simple HF-calculations are:

- The ZPVE (Zero Point Vibrational Energy).
- Anharmonicity in the vibrational potential energy surface.
- Basis sets are too small.
- Neglect of electron correlation.
- The Hartree-Fock potential is too steep and therefore frequencies are too high.

In general, the calculated ab initio frequencies are overestimated, at the Hartree-Fock level by about 10-20%, and at the MP2 level by about 5-10%. This overestimation in the frequencies also depends on the type of vibrational mode and on the frequency range, varying between 1 and 12%. Thus for modes that appear at high frequency, the difference between the harmonic oscillator prediction and the exact or Morse potential like behavior is about 10%. However at a very low frequency, below a few hundred wave numbers, this difference can be off by a large amount.

Several results reported with ab initio and DFT methods are collected in Table 4. The third column is the mean percentage deviation of theoretical harmonic frequencies from experimental fundamentals. The fourth column refers to the ratio $\nu^{exp.}/\omega^{th.}$ between the experimental and calculated frequencies, i.e. the scale factor.

Table 4. Errors obtained in the calculated frequencies at several ab initio levels

level	no. molecules	% error	scale factor, λ	ref.
HF/3-21G	38	12	0.89	31
HF/6-31G*	36	13	0.8929	32
MP2-fu/6-31G*	36	7	0.921	32
			0.96[b]	33
			0.94[c]	33
B-LYP/6-31G*	20	26[a]	0.990	34
B3-LYP/6-31G*		19[a]	0.963	34

[a]rms deviation, in cm^{-1}. [b]For the first-row molecules. [c]For the second-row molecules.

In benzene molecule, the error with the different DFT and ab initio levels can be observed in Fig. 2. The errors in aniline molecule are shown in Fig. 3 and in Table 5. The values are listed in Table 5. It is noted that the calculations at the HF level, fail to give the observed experimental pattern. Inclusion of electron correlation slightly improves the computed frequencies. Only with density functional methods the frequencies are close to the experimental. However, these results have not adequately reproduced all the experimental pattern of frequencies and intensities. The use of scale factors, solves this problem.

The relative accuracy of the results obtained, at some chosen computational level, is better than the absolute accuracy[11]. On this basis, Fig. 1 sketches the error in some one kind of parameter (e.g. a vibrational mode), as computed in a variety of molecular environments, with different methods and sized basis sets. The vertical axis shows the difference between the true value in a given molecule of some particular vibrational mode, and the value computed with different methods and various sizes of SCF basis sets. The errors in computing the chosen vibrational mode in many different molecules are found to fall within the shaded area of the diagram. The HF convergence limit, approached by very large basis sets, still differs from the true value, but this residual error has been found empirically to be remarkably constant for a given parameter, and is very nearly independent of the molecule studied. The calculations can be done efficiently[11] at the point marked "X" in Fig. 1, and this residual error can be removed with the use of scale factors, and therefore give rise to an accurate predicted frequency.

Table 5. Errors obtained in the calculated and scaled wavenumbers of the aniline ring modes by the different procedures, methods and levels

	calculated wavenumbers					scaled wavenumbers with an overall factor					scaled wavenumbers with two scaling equations					scaled wavenumbers with specific scale factors				
				largest error					largest error					largest error					largest error	
Method	rms	MAD	stdDev	positive	negative	rms	MAD	stdDev	positive	negative	rms	MAD	stdDev	positive	negative	rms	MAD	stdDev	positive	negative
SCF																				
HF/6-31G*	16.4	138.5	88.7	320 (7b)		30.9	21.5	22.2	25 (5)	104 (14)	23.9	16.6	17.3	39 (8a)	87 (14)	8.5	6.0	6.0	18 (7b)	28 (20b)
HF/6-31G**	15.8	132.8	83.0	307 (7b)		31.2	21.8	22.3	28 (5)	105 (14)	24.3	16.8	17.5	40 (8b)	90 (14)	9.1	6.9	6.8	23 (7b)	27 (20b)
HF/6-31++G**	15.6	130.7	84.6	309 (7b)							24.3	16.7	17.7	41 (5)	90 (14)	9.2	6.6	6.3	22 (7b)	27 (20b)
Post SCF																				
MP2/6-31G*	9.6	78.2	62.5	185 (7b)	23 (1)	6.2	4.6	7.2	67 (14)	2.2 (1)	5.4	3.9	3.8	9.9 (14)	19.2 (1)	2.5	1.9	1.6	3.9 (12)	6.2 (13)
Density functional																				
B3P86/6-31G*	6.9	49.0	49.1	160 (7b)	9 (10b)	18.2	13.7	11.9	39 (7b)	60 (11a)	13.1	10.3	8.0	24 (18b)	33 (11a)	11.1	8.0	7.6	27 (8a)	27 (20b)
B3P86/6-31G**	6.7	46.2	48.4	159 (7b)	5 (15)	19.1	14.8	12.0	38 (7b)	45 (11a)	13.4	11.3	7.2	26 (8a)	26 (11a)	10.1	7.6	6.6	20 (8a)	27 (20b)
B3LYP/6-31G*	6.1	43.4	42.5	145 (7b)	10 (11a)	16.9	13.8	9.7	23 (7b)	46 (11a)	11.8	8.5	8.2	29 (18b)	32 (11a)	10.8	7.7	7.6	28 (18b)	30 (20b)
B3LYP/6-31G**	5.9	41.3	41.8	143 (7b)	4 (15,11a)	18.6	15.5	10.1	21 (7b)	45 (10a)	11.2	8.5	7.2	22 (18b)	26 (11a)	12.5	9.0	8.7	37 (8a)	27 (20b)
B3LYP/6-311G(2d,p)	19.2	34.6	35.0	124 (7b)	9 (11a)						11.5	8.8	7.3	25 (18b)	27 (11a)	10.7	7.7	7.7	27 (18b)	26 (20b)
B3LYP/6-311++G(2d,p)																				
B3LYP/6-311++G(2d,p)	19.6	33.0	37.0	128 (7b)	11 (8a)						12.4	10.0	7.3	26 (18b)	24 (8a)	11.9	8.5	8.6	25 (18b)	31 (20a)
B3PW91/6-31G**	6.4.7	44.5	47.0	156 (7b)	5 (15)	18.8	14.9	11.5	19 (7b)	44 (11a)	12.8	10.4	7.4	25 (8a)	26 (11a)	10.2	7.7	6.7	20 (7b,8a)	26 (20b)

[illegible] From Ref. 13. From Ref. 14. From Ref. 15. [illegible] = 0.05 in Ref. 17. From Ref. 17.

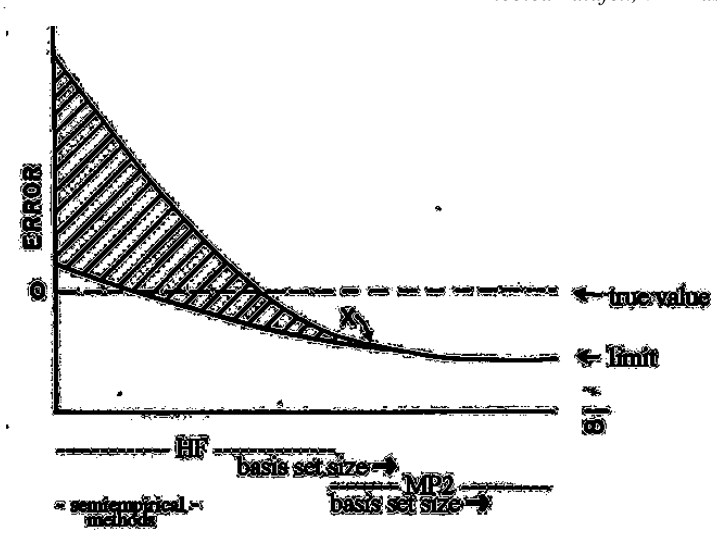

Fig. 1. Schematic representation of the error in calculating a chosen vibrational mode of a molecule in a variety of molecular environments. For wide families of systems, the error is expected to fail within the shaded area.

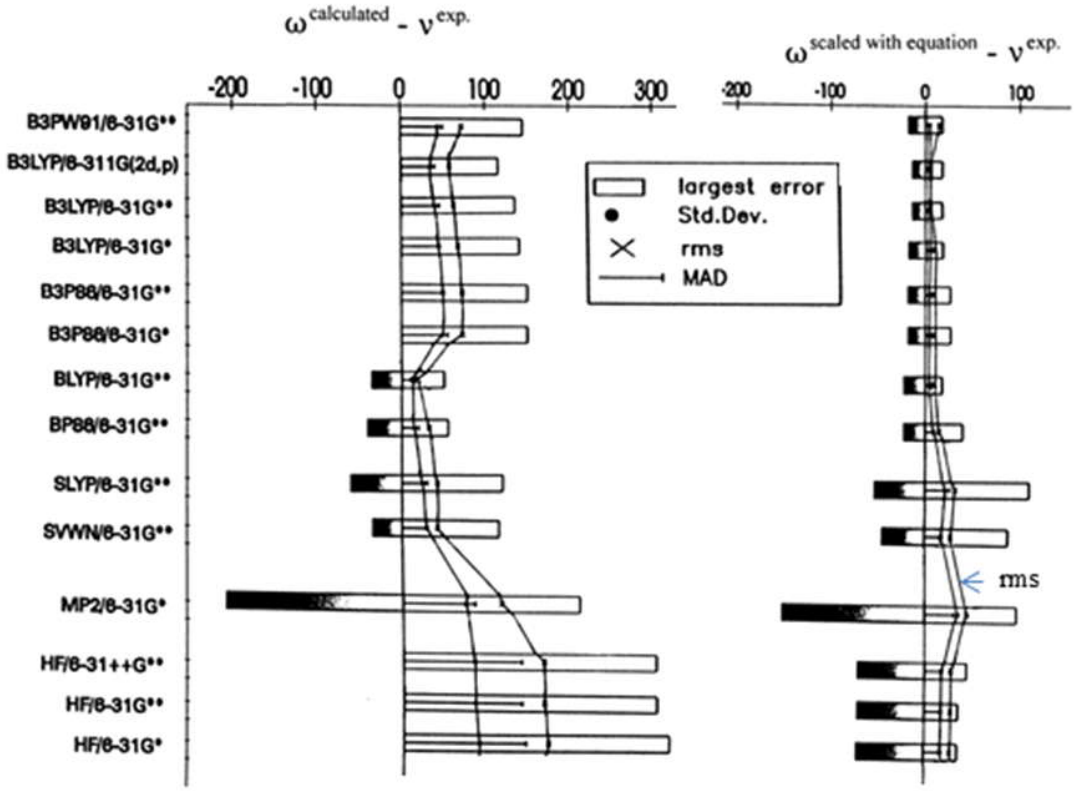

Fig. 2. Error obtained by the different methods and levels in the calculated wavenumbers of the ring modes and in their scaled wavenumbers using a scaling equation.

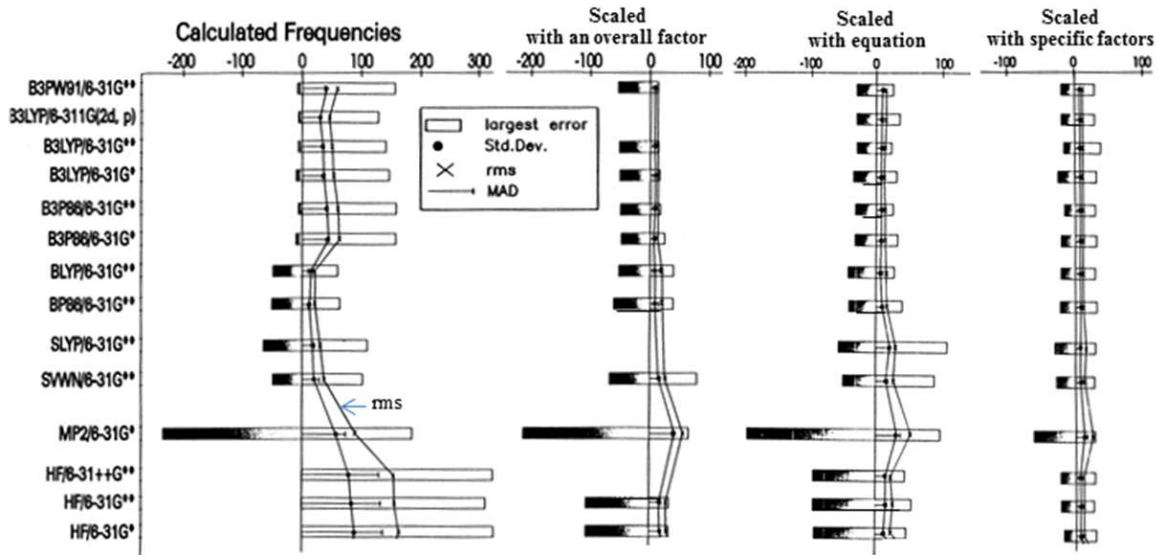

Fig. 3. Error obtained by the different methods and levels in the calculated wavenumbers of the ring modes and in their scaled wavenumbers using an overall scale factor, a scaling equation, and specific scaled facrtors for each mode.

7. Scaling Procedures for the Frequencies

The values of the frequencies are close among similar molecules and characteristic groups. Based on this assumption, three kind of procedures are used for an accurate scaling of the calculated frequencies.[18-20]

7.1 With a single overall scale factor for the calculated level

With this procedure all the computed frequencies of a molecule at a specific level of theory are scaled with a unique scale factor (or correction factor), which is common for all the molecules with the same level of calculation. The correction factors are different for distinct levels of theory, and with low level of calculations, it is necessary to use scale factors far from the value 1.

The procedure to determine this scale factor is complicated, because the scaling factor depends upon not only the basis set or theoretical method used but also the group of molecules used for comparison and whether or not the comparisons are made with only harmonic frequencies or with all fundamentals. The procedure for calculating the scale factor[21] is as follows: With a full set of theoretical frequencies $\omega_i^{th.}$ for different molecules, and with their corresponding experimental fundamental frequencies, $v_i^{expt.}$, the scaling factors λ are those that minimize the residuals.

$\Delta = \Sigma\ (\lambda\ \omega_i^{th.} - v_i^{expt.})^2$ and thus, $\lambda = \Sigma\ \omega_i^{th.}\ v_i^{expt.} / \Sigma\ (\omega_i^{th.})^2$.

Therefore, for the different levels of theory, the scale factors of the 2nd and 5th columns of Table 6 have been reported[21] from a dataset containing 122 molecules and 1066 frequencies.

To minimize the large errors in frequencies at the low end of the frequency range, an inverse frequency scaling factor, λ', is used to minimize the residual, 3rd and 6th columns of Table 6. With these two scale factors, for high and low frequency ranges, have been calculated in the aniline ring modes[22]: the root-mean-square (RMS) errors for the frequencies, the mean absolute deviation (MAD), the standard deviation (Std. Dev.), and the greatest positive and negative deviations from experiment, the 7th to 11th columns, respectively, of Table 5 at different methods and levels.

Table 6. Scale factors at different levels

Level of theory	Scale factor λ	Scale factor λ′[a]	Level of theory	Scale factor λ	Scale factor λ′[a]
HF/ 3-21G	0.9085	1.0075	QCISD-fc/6-31G*	0.9538	1.0147
HF/ 6-31G*	0.8953	0.9061			
HF/6-31+G*	0.8970	0.9131	SVWN/ 6-31G*	0.9833	1.0079
HF/6-31G**	0.8992	0.9089	B-LYP/ 6-31G*	0.9945	1.0620
HF/6-311G**	0.9051	0.9110	B-LYP/6-311G(df,p)	0.9986	1.0667
HF/6-31G(df,p)	0.9054	0.9085	B-P86/6-31G*	0.9914	1.0512
			B3-LYP/ 6-31G*	0.9614	1.0013
MP2-fu/ 6-31G*	0.9427	1.0214	B3-P86/6-31G*	0.9558	0.9923
MP2-fc/ 6-31G*	0.9434	1.0485	B3-PW91/6-31G*	0.9573	0.9930
MP2-fc/6-31G**	0.9370	1.0229			
MP2-fc/6-311G**	0.9496	1.0127			

[a]Suitable for the prediction of low-frequency vibrations 1/λ.

An analysis of Table 6 give rises to the following conclusions: In the fundamental frequencies, the most cost-effective procedures found for predicting vibrational frequencies are the B3-based/6-31G* DFT procedures, with the lowest rms values. The B-based DFT procedures are not performing quite as well as the corresponding B3-based procedures, and for this reason, they were omitted in Table 5. MP2/6-31G* does not appear to offer a significant improvement in performance over HF/6-31G* and occasionally shows a high degree of error. While the QCISD method yields frequencies (not shown in Table 5) that are more reliably predicted than those computed at the MP2 level, the improvement comes at a significant additional computational cost and, the results are generally not better than those for the much less expensive B3-based DFT procedures.

With low-frequency vibrations the DFT methods also yield to the lowest errors, while HF performs slightly worse.

An overall conclusion is that B3-based DFT procedures provide a very cost-effective means of determining harmonic vibrational frequencies and derived thermochemical quantities. They show fewer poorer cases than do HF- and MP2-based procedures. With ab initio methods, although the error is remarkable reduced using a single overall scale factor, as compared to the calculated frequencies, in several ring modes of the aniline molecule the error is very large yet. With DFT procedures, however, the errors are in general very small and can be used efficiently a single overall scale factor.

7.2 With a scaling equation

This procedure uses a scaling equation to correct the computed frequencies of a molecule at a specific level of theory. Therefore slightly improved in the predicted frequencies should be expected, especially in the low-frequency region, than when a unique scale factor is used. The scaling equation can also refer to a group or to a kind of molecules for a specific level of theory, which greatly improves the accuracy in the predicted frequencies.

Fig 4 is an example with the benzene ring modes. By fitting, the scaling equation is obtained. Table 7 collects the calculated scaling equations obtained in the benzene[23] and uracil[24] molecules, as well as in the amino modes.

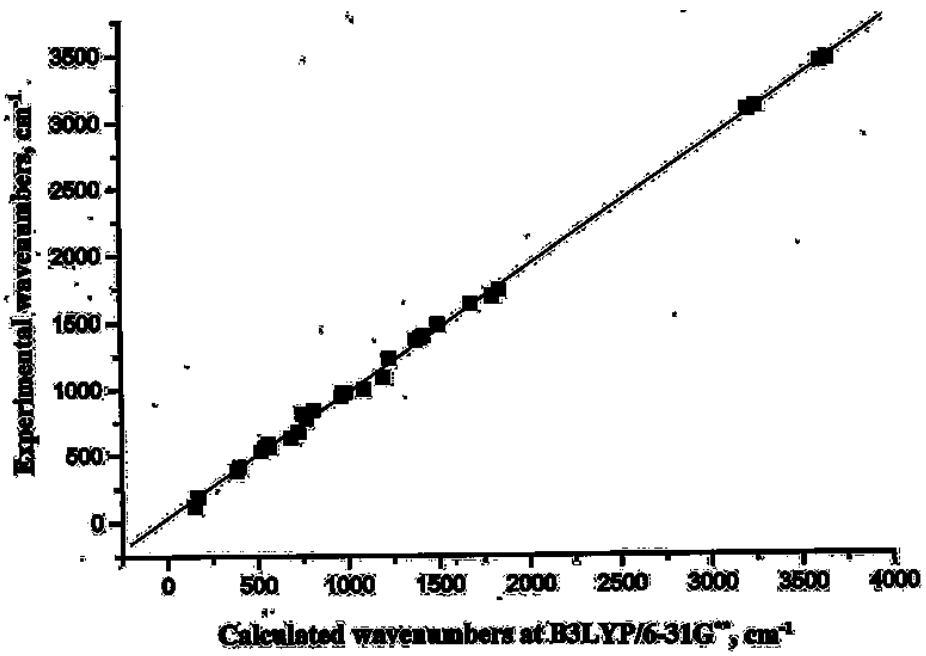

Fig. 4. Calculated frequencies by B3LYP/6-31G** versus experimental ones in benzene molecule.

Table 7. Scaling equations $\nu^{scaled} = a + b \cdot \omega^{calculated}$ for the ring modes of benzene and uracil derivatives

Methods	benzene		uracil		amino modes	
	a	b	a	b	a	b
HF/6-31G*	-4.0	0.9103	4.6	0.8924	22.7	0.8934
HF/6-31G**	-8.6	0.9162	5.7	0.8867	40.3	0.8846
HF/6-31++G**	-6.2	0.9153	10.5	0.8938	45.9	0.8833
MP2/6-31G**	83.4	0.9088				
MP2/6-311G**	97.3	0.9156				
BP86/6-31G**	32.7	0.9752	46.0	0.9678	44.3	0.9699
BP86/6-311G(2d,p)	28.8	0.9819				
BLYP/6-31G**	27.2	0.9791	46.4	0.9718	31.3	0.9791
B3P86/6-31G*	25.0	0.9473	29.9	0.9412	33.0	0.9434
B3P86/6-31G**	27.2	0.9476	34.1	0.9389	57.4	0.9318
B3LYP/6-31G*	23.3	0.9519	30.8	0.9468	21.3	0.9555
B3LYP/6-31G**	22.1	0.9543	34.6	0.9447	44.5	0.9441
B3LYP/6-311G(2d,p)	18.6	0.9616			24.5	0.9572
B3LYP/6-311+G(2d,p)	20.8	0.9601	30.8	0.9538	45.0	0.9484
B3LYP/6-311++G(2d,p)	28.5	0.9574			45.6	0.9482
B3LYP/6-311++G(3df,pd)			31.9	0.9512		
B3LYP/aug-cc-pVDZ			28.6	0.9543		
B3LYP/DGDZVP			39.2	0.9472		
B3PW91/6-31G**	24.8	0.9501	34.9	0.9393	56.8	0.9325
B3PW91/6-311+G(2d,p)	25.2	0.9554				
MPW1PW91/6-311+G(2d,p)	24.6	0.9499				

With these equations have been calculated in the aniline ring modes the RMS errors, the MAD and the Std. Dev. for the frequencies, and the greatest positive and negative deviations from experiment, the 12^{th} to 16^{th} columns, respectively, of Table 5 at different methods and levels.

A significant improvement is reached in DFT methods with a reduction of 33% the error over the use of the overall scale factor (rms of 24.3 at HF/6-31G** level versus 11.2 at B3LYP/6-31G**).

With the use of the scaling equation approach, the low wavenumber vibrations are usually predicted fairly accurate while stretching wavenumbers appear someone overestimated. By dividing the wavenumber range into two parts, and using one scaling equation for the 0-2000 cm^{-1} range and another one for the 2000-4000 cm^{-1} range, the error in the stretching region is slightly reduced.

7.3 With a specific scale factor for each mode

It is well known that in organic molecules many of the vibrational modes are localized and that many functional groups have characteristic frequencies that do not vary much between different molecules. Therefore, considering groups of similar molecules can be calculated correction factors (or scaling factors)

$$\lambda = \nu^{exp.}/\omega^{th.} \text{ (or } \lambda' = \omega^{th.}/\nu^{exp.})$$

that brings the computed frequencies in line with the available experimental data. That is, the procedure is based on the assumption that the ratios between experimental and computed frequencies are fairly constant for each type of characteristic frequency, such as C-H stretch, C-Cl stretch, NH_2 torsion, etc. It is then possible to derive for known experimental spectra a correction factor for each characteristic frequency by taking the average of the ratios between the experimental and computed frequencies, λ, and to use them for predicting or assigning unknown spectra.

The introduction of different scale factors for distinct types of vibrational modes remarkably improves the accuracy of the predicted frequencies. The introduction of a scaling factor for a single characteristic frequency is capable of accounting for all the deficiencies of the quantum chemical methods and leads to a more precise prediction for specific characteristic frequencies that are of special interest.

It should be noted that certain types of vibrational modes are much more readily identified than others, e.g. the stretchings. On the other hand, many of the torsion and out-of-plane modes are delocalized throughout a wide low-frequency range, and it is difficult to identify these modes or to differentiate between them. Thus, the scale factors obtained with these modes produce many errors, and should be considered with caution.

Table 8 collects the calculated specific scale factors obtained in the benzene[23] molecule, while Table 9 lists the values obtained in uracil[24] modes. With the specific scale factors of Table 8 have been calculated in the aniline ring modes the RMS errors, the MAD and the Std. Dev. for the frequencies, and the greatest positive and negative deviations from experiment, the last five columns of Table 5, at different methods and levels.

In Fig. 5 can be seen in graphical forms the differences in the scaled frequencies with the three scaling procedures described above. DFT methods always give the best results. The errors with the scaling equation procedure are slightly lower than with the overall factor procedure, especially in DFT methods. MP2 frequencies give the worst results and they should not be scaled with these procedures. Finally, the specific factor lead to the best results, although it requires much more effort, and a previous assignment of the calculated bands.

Table 8. Calculated specific scale factors, exp./ cal., for each normal mode of the benzene molecule, and at some of the levels considered

Ring mode Wilson no.	HF/ 6-31G**	MP2/ 6-31G**	B3LYP/6 -31G*	B3LYP/6 -31G**	B3LYP/ 6-311+G(2d,p)	B3PW91/6- 31G**	B3PW91/ 6-311+G(2d,p)
1	0.9169	0.9660	0.9726	0.9736	0.9825	0.9679	0.9741
2	0.9113	0.9363	0.9564	0.9582	0.9638	0.9552	0.9606
3	0.8994	0.9670	0.9733	0.9775	0.9715	0.9818	0.9788
4	0.9088	1.4140	0.9846	0.9846	0.9905	0.9833	0.9910
5	0.8715	1.0772	0.9802	0.9773	0.9857	0.9754	0.9870
6	0.9145	0.9841	0.9777	0.9792	0.9739	0.9840	0.9821
7	0.9147	0.9382	0.9591	0.9609	0.9659	0.9576	0.9628
8	0.8919	0.9558	0.9662	0.9780	0.9807	0.9621	0.9729
9	0.9144	0.9623	0.9750	0.9790	0.9822	0.9790	0.9839
10	0.8814	0.9920	0.9804	0.9793	0.9850	0.9782	0.9857
11	0.8821	0.9782	0.9725	0.9712	0.9839	0.9711	0.9861
12	0.9216	0.9902	0.9902	0.9922	0.9802	0.9970	0.9869
13	0.9178	0.9412	0.9619	0.9638	0.9688	0.9607	0.9660
14	0.9699	0.8925	0.9642	0.9656	0.9847	0.9502	0.9683
15	0.9637	0.9573	0.9702	0.9743	0.9778	0.9760	0.9810
16	0.8786	1.0076	0.9590	0.9590	0.9660	0.9660	0.9750
17	0.8775	1.0556	0.9979	0.9929	0.9891	0.9888	0.9896
18	0.9116	0.9596	0.9712	0.9730	0.9812	0.9694	0.9768
19	0.9016	0.9630	0.9693	0.9731	0.9782	0.9737	0.9792
20	0.9117	0.9360	0.9567	0.9585	0.9638	0.9552	0.9605

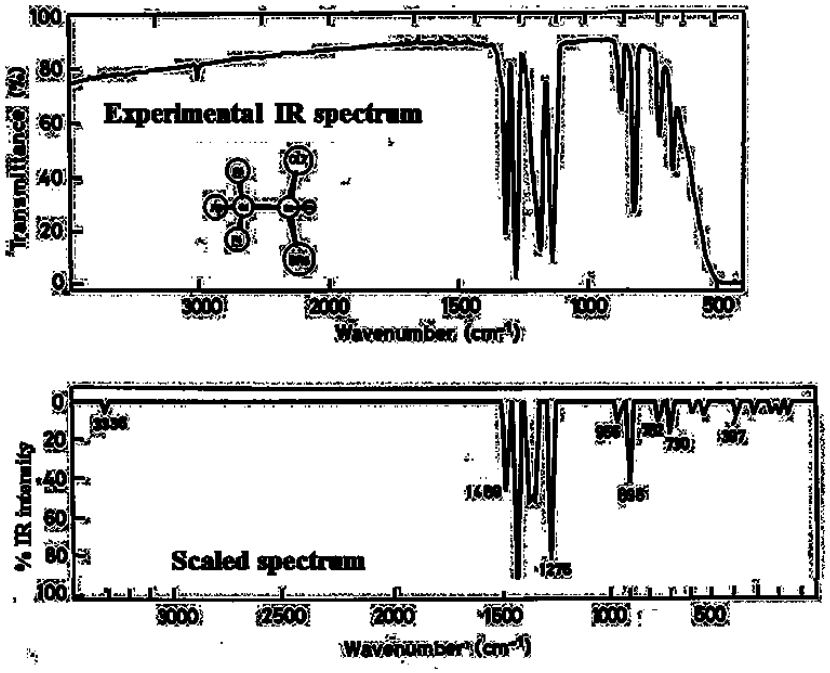

Fig. 5. Experimental IR and scaled IR spectra of halothane molecule.

Table 9. Calculated specific scale factors, exp./ cal., for each normal mode of the uracil molecule, and at some of the levels considered

Ring mode	MP2/ 6-31G*	B3P86/ 6-31G**	B3LYP/ 6-31G*	B3LYP/ 6-31G**	B3PW91/6-31G**
2	1.1491	1.0819	1.0882	1.0882	1.0819
3	1.0209	1.0156	1.0156	1.0156	1.0156
4	1.0422	0.9950	1.0000	0.9975	0.9975
5	0.9884	0.9865	0.9865	0.9865	0.9884
6	0.9908	0.9871	0.9889	0.9908	0.9889
7	0.9982	0.9982	1.0000	1.0018	1.0000
8	0.9629	0.9545	0.9715	0.9680	0.9561
9	0.9456	0.9524	0.9579	0.9607	0.9538
10	0.9169	0.9795	0.9822	0.9835	0.9808
11	1.0485	0.9960	1.0066	1.0066	0.9974
12	1.0596	1.0013	1.0116	1.0129	1.0038
13	1.0037	0.9853	0.9865	0.9865	0.9853
14	0.9616	0.9764	0.9835	0.9865	0.9814
15	1.0452	1.0010	1.0031	1.0021	0.9990
16	0.9910	0.9960	0.9980	1.0000	0.9970
17	0.9641	0.9772	0.9799	0.9835	0.9781
18	0.9482	0.9686	0.9742	0.9783	0.9694
19	0.9324	0.9573	0.9588	0.9643	0.9596
20	0.9597	0.9769	0.9755	0.9812	0.9776
21	0.9659	0.9788	0.9809	0.9858	0.9802
22	0.9662	0.9804	0.9790	0.9845	0.9818
23	0.9512	0.9612	0.9663	0.9701	0.9624
24	0.9585	0.9630	0.9699	0.9710	0.9647
25	0.9534	0.9514	0.9624	0.9629	0.9534
26	0.9400	0.9400	0.9512	0.9518	0.9421
27	0.9427	0.9511	0.9529	0.9550	0.9520
28	0.9455	0.9521	0.9556	0.9571	0.9530
29	0.9513	0.9432	0.9536	0.9492	0.9434
30	0.9529	0.9462	0.9571	0.9524	0.9465

8. Comparison of the different methods

The majority of the published works with ab initio methods use a single overall correction value for the frequencies, with no consideration for the different modes. Sometimes a simplification is used with only two or three scale factors for the modes, e.g., 0.9 for stretches and bends and 1.0 for torsion. However the best accuracy is obtained if a specific scale factor is used for each mode and level of calculation, although it requires slightly more effort. The only scale factors reported with this procedure, to our knowledge, are for tertiary amines[25], and for toluene molecule[26].

However, the scale factors reported for toluene, are not enough detailed as the calculations carried out by us on the benzene molecule, and listed in Table 8, with a specific scale factor for each ring mode, numbered according to Wilson notation[23].

DFT methods and at 6-31G** level, shows a more reliable prediction for the calculated frequencies (with scale factors more close to the unit) than with more expensive HF and MP2 methods. Table 10 lists our calculated results in several benzene derivatives, as well as in uracil derivatives. A detailed description of these results can be seen in the following references: benzene[23], aniline[22], benzoic acid[27], 1,4-dicyanobenzene and 2,4-difluorobenzonitrile [28], uracil [24], 5-fluorouracil 29], 5-bromouracil, 5-methyluracil (thymine)[30], 2-thiouracil[31]. Also different halo-uracil derivatives[32] and 5-aminouracil molecule[33] have been studied using the scaling equation procedure.

Table 10. RMS errors obtained in the calculated and scaled wavenumbers of several benzene and uracil derivatives at the B3LYP/6-31G** level.

Molecules	(a)	(b)	(c)	(d)
benzene	62	17	8.8	-
aniline	60	19	12.4	11.0
benzoic acid	55.9	19.7	13.9	10.7
phenylsilane	60.1	17.0	10.7	10.5
p-aminobenzoic acid	47.8	19.3	13.7	11.3
p-methoxybenzoic acid	46.3	18.6	13.4	12.5
1,4-dicyanobenzene	56.5	23.1	17.7	13.4
2,4-difluorobenzonitrile	64.1	20.2	16.5	14.2
Phenothiazine	75.0	24.2	17.6	17.1
uracil	66.4	21.4	13.8	-
5-fluorouracil	70.3	29.8	23.5	14.7
5-bromouracil	76.2	29.2	18.5	13.7
5-methyluracil	59.8	21.5	18.4	13.1
5-nitrouracil	71.7	26.1	16.5	13.0
1-methyluracil	69.2	27.0	17.9	15.8
2-thiouracil	79.0	26.5	15.5	11.5
3-methyluracil	63.2	22.8	15.6	11.0
1,3-dimethyluracil	49.4	23.1	16.5	12.1

When the comparisons theory-experiment are carried out with experimental values in the gas phase, the concordance is very high. Fig. 5 shows as example the experimental IR spectrum in gas phase of the general anesthetic halothane versus the scaled IR spectrum.[34] Can be seen that the concordance appear in the scaled frequency values, as well as in the calculated IR intensities of the bands.

However, in the solid state the differences are higher. Fig. 6 shows as example the experimental Raman spectra of 5-bromouracil molecule[35]. Although the scaled frequencies appear close to the experimental ones, however, the calculated intensities of the bands are very different of those in the experimental spectrum. This happen when the intermolecular H-bonds in the crystal have some relevance. In these cases, the solid state should be better simulated. One approach is through a dimer, trimer or tetramer forms, according to that observed by x-ray.

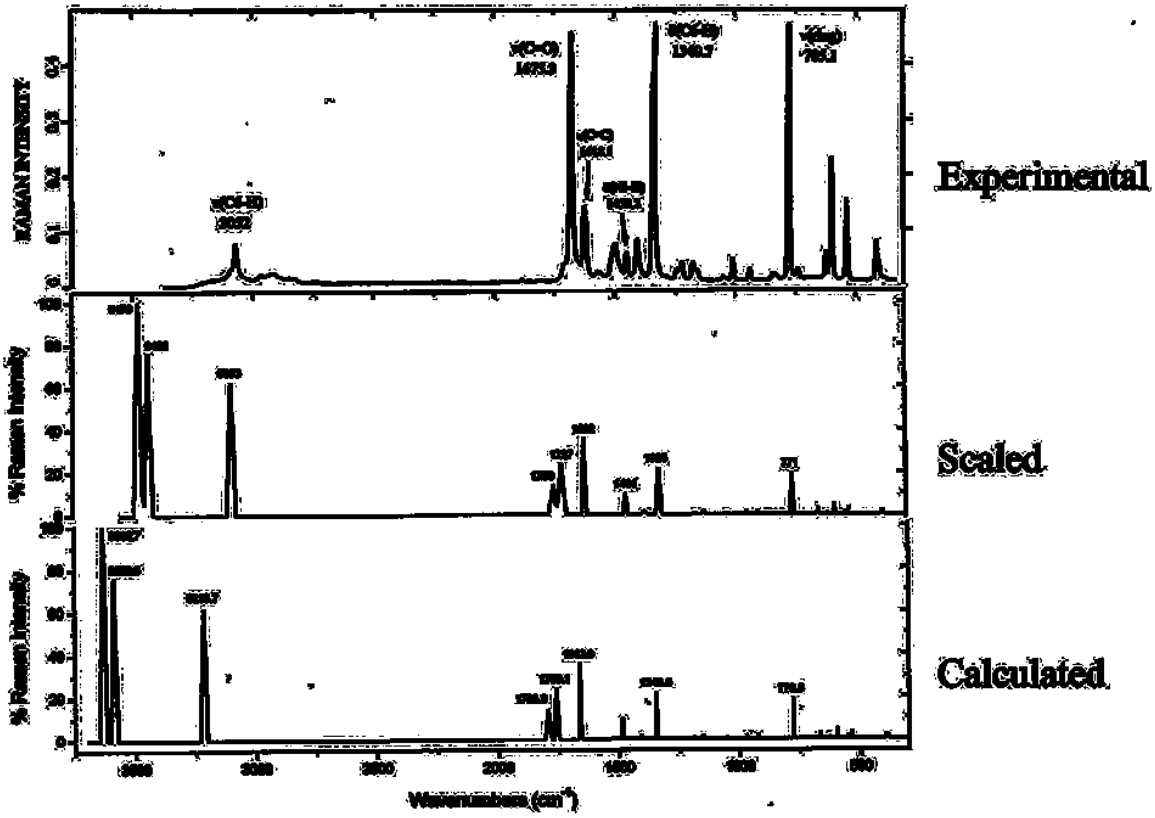

Fig. 6. Comparison of the experimental Raman spectrum of 5-bromouracil in the solid state with those spectra simulated (calculated and scaled theoretically) at the B3LYP/6-311+G(2d,p) level. The scaled spectrum was carried out with the two-scaling equation procedure.

An example of this simulation is presented in Fig. 7, which shows the results in 5-iodouracil molecule, in its monomer[36] and tetramer[37] forms. Three kinds of tetramer forms were simulated trying to reproduce the unit cell. The pattern of the scaled IR spectrum with the tetramer forms appears much more close to the experimental spectrum than with its monomer form. For clarity, in the figure was also included the assignment of the most intense IR bands. The numbers refers to the notation used for the uracil ring modes[24].

9. Conclusions

The procedure selected for scaling depends on the size of the organic molecule and the accuracy required for the predicted frequencies.

Among the procedures for scaling the frequency, the CCD, CCSD(T) and QCISD methods and large basis sets give rise to almost corrected harmonic frequencies. Thus it is not necessary to use scaling procedures. However, these methods are very expensive in time and memory computer consuming, and are limited to molecules with less than 4 atoms.

With larger organic molecules, but less than 20 carbon atoms, HF, MP2 and DFT methods and large basis sets can be used for calculating frequencies. If the accuracy required is not very high (the errors in the predicted frequencies could be between 0-4%), then the use of a unique scale factor with the calculated frequencies (or two, for the high and for the low-frequencies vibrations), is the simplest and

easiest procedure. In this case, among the HF, MP2 and DFT methods, the most cost-effective are the HF/6-31G* and the B3-based/6-31G*. If the accuracy required is high, then, at the same level, previous scale factors should be calculated for each mode from related and simpler molecules.

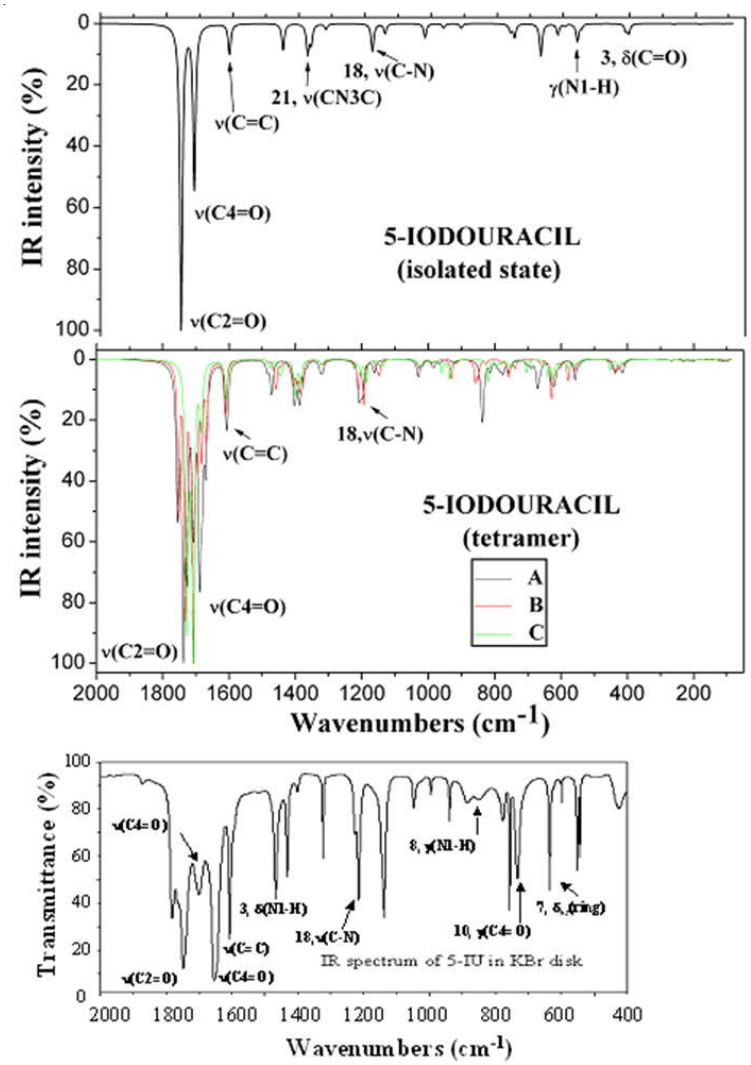

Fig. 7. Comparison of the experimental IR spectrum of 5-iodouracil in the solid state with those spectra simulated (scaled theoretically) considering a monomer (isolated stated) and a tetramer form, at the B3LYP/DGDZVP level. Three kind of tetramer forms were simulated, named A, B and C.

In Benzene, the predicted frequencies for the ring modes using DFT methods leads to very small errors. Thus in this molecule and in small derivatives, the DFT methods should be used.

With molecules between 20–40 carbon atoms, HF and DFT methods can be used for calculating frequencies. However, the cost/effective ratio with HF is higher than with DFT methods. Thus, DFT methods should be only used. With very large molecules, higher than 40 carbon atoms, semiempirical methods are recommended to be used, in special AM1. With these methods, the specific scale factor procedure for each mode should be used, which gives good predicted frequencies, with error lower than 5%.

References

1. Young D.C., Computational Chemistry. *A practical Guide for Techniques to real-world problems*. J. Wiley & Sons, New York, 2001.
2. F. Jensen, *Introduction to Computational Chemistry*, J. Wiley & Sons, New York, 1999.
3. W. Koch, M.C. Holthausen. *A Chemistry's Guide to Density Functional Theory*. Wiley –VCH, Weinheim, 2000
4. R.G. Parr, W. Wang. *Density-functional theory of atoms and molecules*. Oxford Univ. Press, Oxford 1989.
5. Becke, A.D., *Phys. Rev*. **A38** (1988) 3098.
6. Lee, C., Yang, W. & Parr, R.G., *Phys. Rev.* **B37** (1988) 785.
7. Becke, A.D., *J. Chem. Phys.* **97** (1992) 9173; & *J. Chem. Phys.* **98** (1993) 5648.
8. Perdew, J.P., *Phys. Rev*. **B33** (1986) 8822; & **B34**, 7406 (E).
9. (a) Perdew, J.P. & Wang, Y., *Phys. Rev.* **B45** (1992) 13244.
   (b) Perdew, J.P., Chevary, J.A., Vosko, S.H., Jackson, K.A., Pederson, M.R., Singh, D J, Fiolhais C., *Phys. Rev.* **B46** (1992) 6671.
10. M. Alcolea Palafox, *Recent Research Developments in Physical Chemistry*, **2**, 213-232 (1998), Ed.: Transworld Research Network, Kerala (India)
11. Boggs, J.E., *Phys. Chem. Minerals*, **14**, 407; & 1988, *Pure & Appl. Chem*. **60** (1987) 2, 175.
12. Castell-Ventura, M. & Kassab, E., *Spectrochim. Acta*, 50A, 1 (1994) 69.
13. Fukuyo, M.; Hirotsu, K. & Higuchi, T., *Acta Crystallog*. 38B, 2 (1982) 640.
14. Lister, D.G.; Tyler, J.K.; Hog. J.H. & Larsen, N.W. *J. Molec. Struct.* 23 (1974) 253.
15. Schultz, G.; Portalone, G.; Ramondo, F.; Domenicano, A. & Hargittai, I. *Struct. Chem*. 7(1996)59.
16. Pliva, J.; Johns, J.W.C. & Goodman, L., *J. Molec. Spectrosc.* 148, 2 (1991) 427.
17. Roussy, G. & Nonat, A., *J. Molec. Spectrosc.* 118 (1986) 180.
18. Palafox M A, V.K. Rastogi, *Perspectives in Modern Optics & Optical Instrumentation*, pp. 91-98 (2002). Ed: J. Joseph, A. Sharma, V.K. Rastogi. Anita Publications.
19. M. Alcolea Palafox, J.L. Núñez, M. Gil, V.K. Rastogi, *Perspectives in Engineering Optics*, pp. 356-391 (2002). Ed: K. Singh, V.K. Rastogi. Anita Publications.
20. M. Alcolea Palafox, V.K. Rastogi. *Perspectives in Engineering Optics and Spectroscopy*, (2006). Ed: Anita Publications.
21. Scott, A.P. & Radom, L., *J. Phys. Chem.* **100** (1996) 16502.
22. (a) Alcolea Palafox, M.; Núñez, J.L. & Gil, M. *J. Molec Struct (Theochem)*, **593** (2002) 101. (b) Alcolea Palafox, M.; Gil, M.; Núñez, J.L.; Rastogi, V.K.; Mittal, L. & Sharma R., *Int J. Quantum Chem*, **103,** 4 (2005) 394.
23. Alcolea Palafox, M. *Int J. Quantum Chem*, **77** (2000) 661.
24. Alcolea Palafox, M. & Rastogi, V.K. *Spectrochim Acta,* **58A** (2002) 411. (b) Alcolea Palafox, M.; Iza, N. & Gil, M. *J. Molec Struct (Theochem)*, **585** (2002) 69.
25. a) Hameka, H.F., Famini, G.R., Jensen, J.O. & Newhouse, E.I., *Gov. Rep. Announce Index*, **90** (1990) 13. b) Hameka, H.F., Famini, G.R., Jensen, J.O. & Jensen, J.L., *Gov. Rep. Announce Index*, **91** (1991) 15.
26. Hameka, H.F. & Jensen, J.O., *J. Mol. Struct. (Theochem.)*, **362** (1996) 325.
27. Alcolea Palafox, M.; Núñez, J.L. & Gil, M. *Int J. Quantum Chem*, **89** (2002) 1.
28. (a) Rastogi, V.K.; Jain, V.; Alcolea Palafox, M.; Singh, D.N. & Yadav, R.A. *Spectrochim Acta*, **57A** (2001) 209. (b) Alcolea Palafox, M.; Rastogi, V.K.; Singh, C. & Tanwar, R.P. *Spectrochim Acta*, **57A** (2001) 2373. (c) Rastogi, V.K.; Alcolea Palafox, M.; Tanwar, R.P. & Mittal, L. *Spectrochim Acta,* **58A** (2002) 1987. (d) Alcolea Palafox, M.; Rastogi, V.K. & Mittal, L. *Int J. Quantum Chem*, **94** (2003) 189. (e) Alcolea Palafox, M.; Rastogi, V.K. & Vats, J.K. *J. Raman Spectrosc*, **37** (2006) 85. (f) Alcolea Palafox, M.; Rastogi, V.K.; Mittal, L.; Kiefer, W. & Mital, H.P. *Int J. Quantum Chem,* **106** (2006) 1885. **(g)** Rastogi, V.K.; Alcolea Palafox, M.; Singhal, S.; Ojha, S.P. & Kiefer, W. *Int J. Quantum Chem,* **107**, 5 (2007) 1099.

29. Rastogi, V.K.; Jain, V.; Yadav, R.A.; Singh, C. & Alcolea Palafox M., *J. Raman Spectrosc*, **31** (2000) 595. (b) Alcolea Palafox, M.; Rastogi, V.K.; Kumar, H.; Kostova, I. & Vats J.K., *Spectrochim Acta Part A: Molec. Biomol. Spectrosc*. **79** (2011) 970.
30. Rastogi V.K.; Singh, C.; Jain, V. & Alcolea Palafox M., *J. Raman Spectrosc*, **31** (2000) 1005.
31. Alcolea Palafox, M.; Rastogi, V.K.; Tanwar R.P. & Mittal, L. *Spectrochim Acta*, **59A** (2003) 2473.
32. (a) Alcolea Palafox, M.; Rastogi, V.K.; Kumar, H.; Kostova, I. & Vats, J.K. *Spectrosc. Letts,* 44 , 4 (2011) 300. (b) Alcolea Palafox, M.; Rastogi, V.K.; Guerrero-Martínez, A.; Tardajos, G.; Joe, H. & Vats, J.K. *Vibra. Spectrosc*, **52** (2010) 108. (c) Alcolea Palafox, M.; Kumar, H.; Sharma, M.; Joe, H. & Rastogi, V.K. *Advancements and Futuristic Trends in Material Science*, (2011) pp. **70-87.** Ed: M. Saleem Khan, & A. Gupta. Allied Publishers Pvt Ltd, New Delhi (India).
33. Alcolea Palafox, M.; Tardajos, G.; Guerrero-Martínez, A.; Rastogi, V.K.; Mishra, D.; Ojha, S.P. & Kiefer, W. *Chem Phys*. **340** (2007) 17.
34. Melendez, F.J. & Alcolea Palafox, M. *J. Mol. Struct. (Theochem.)*, 493 (1999) 179.
35. Rastogi, V.K.; Alcolea Palafox, M.; Mittal, L.; Peica, N.; Kiefer, W.; Lang, K. & Ojha, S.P. *J. Raman Spectrosc*, **38,** 10 (2007) 1227. (b) Alcolea Palafox, M.; Talaya, J.; Guerrero-Martínez, A.; Tardajos, G.; Hitesh, K.; Vats, J.K. & Rastogi, V.K. *Spectrosc Letts*, **43**, 1 (2010) 51.
36. Rastogi, V.K.; Alcolea Palafox, M.; Guerrero-Martínez, A.; Tardajos, G.; Vats, J.K.; Kostova, I.; Schlucker, S. & Kiefer, W. *J. Molec Struct (Theochem)*, **940** (2010) 29.
37. Alcolea Palafox, M.; Rastogi, V.K.; Guerrero-Martínez, A.; Tardajos, G.; Joe, H. & Vats, J.K. *Vibrational Spectrosc*, **52** (2010) 108.